

DOI: 10.1002/adma.200602250

Bio-Functional Mesolamellar Nanocomposites Based on Inorganic/Polymer Intercalation in Purple Membrane (Bacteriorhodopsin) Films**

By Keith M. Bromley, Avinash J. Patil, Annela M. Seddon, Paula Booth, and Stephen Mann*

Fabrication of self-assembled structures using multiple building blocks with diverse functionalities such as biomolecules, polymers and inorganic nanoparticles has attracted considerable interest due to the potential applications of hybrid constructs in biotechnology and bio-electronic devices.^[1,2] A principal candidate biomolecule for incorporation into multi-functional devices is the photoactive protein-retinal complex, bacteriorhodopsin (BR),^[3] which acts as a light-activated proton pump in the purple membrane (PM) of halophilic bacteria. Extracted PM fragments exhibit photoelectric, photochromic and photo-induced proton transport properties, and have been investigated as potential materials for holography, non-linear optics, and optical information processing.^[3,4] PM films are only stable over a limited range of pH, humidity and temperature conditions, and are fragile and difficult to manipulate, which severely limit their application in photoelectric devices.

PM fragments can be readily extracted from halophilic bacteria such as *Halobacterium salinarum* in the form of micron-sized, 5 nm-thick lipid bilayer sheets that consist of a 2D protein/lipid crystalline array of unidirectionally oriented BR molecules. Proton transport from the cytoplasmic to extracellular side of the PM is initiated by light-activated isomerisation of the BR-bound retinal chromophore, and coupled with a thermally activated photocycle involving a series of spectroscopic intermediates (J, K, L, M, N, and O states) associated with deprotonation/protonation of the Schiff-base retinal linkage. A significant blue shift occurs between the protonated ground state (B₅₆₈) and stable unprotonated intermediate (M₄₁₂) that gives rise to photochromism and the possibility of using PM patches in imaging and recording devices such as photochromic inks, holographic interferometry and volumetric memories.^[4] The response to steady state illumination is extremely sensitive and the photocycle can be cycled many

times more than for synthetic materials, as well as enhanced in efficiency by increasing the M lifetime by site-directed mutagenesis (notably replacing Asp96 by Asn96).^[4,5]

Previous research has been undertaken on the incorporation of PM flakes into polymer gels^[6,7] and sol-gel derived glasses^[8–12] in order to produce bulk composite materials for potential photochromic applications. In contrast, the photoelectric response of BR, which depends on a net charge separation (voltage) across the lipid membrane, necessitates the fabrication of films in which PM fragments are uniformly oriented in order to facilitate unidirectional proton transport. Several approaches, involving layer by layer deposition,^[13–15] Langmuir–Blodgett deposition,^[16–19] electrophoretic sedimentation,^[20,21] antibody recognition^[22] and chemisorption self-assembly^[23] have been developed to achieve this objective. The films are generally soft and brittle, and the photoelectric response sensitive to changes in environmental conditions such as pH, temperature and relative humidity.

In this paper, we describe a novel approach for preparing BR-based mesolamellar nanocomposites comprising uniformly oriented sheets of intact PM lipid bilayers intercalated between nanometre-thick layers of amorphous silica (Fig. 1). The method uses a stacked array of PM fragments, typically produced by electrophoretic deposition, as a mesolamellar template that can be readily swelled by reactant solutions such that deposition of aminopropyl-functionalized silica occurs specifically within the inter-layer regions of the lipid film. Although synthetic lipid bilayers have previously been co-assembled with amorphous silica to produce polymerizable chiral mesolamellar tubes with solvatochromic properties,^[24] to the best of our knowledge no studies have used intact lipid membrane assemblages as templates for the construction of bio-functional mesolamellar materials. Significantly, the organosilica/PM mesolamellar films are self-supporting, stable in water for several months, and show retention of both photoelectric and photochromic properties. Moreover, compared with unmodified PM films, the hybrid nanocomposites exhibit an enhanced photoelectric response under conditions of high relative humidity. Finally, we demonstrate the generic significance of our approach by preparing bio-functional organoclay/PM mesolamellar films, as well as polymer/PM layered nanocomposites using macromolecules such as polyvinyl alcohol, poly-L-lysine or chitosan.

BR-based lamellar nanocomposites were fabricated by a simple swelling/drying procedure of multilayer PM films in

[*] Prof. S. Mann, K. Bromley, Dr. A. J. Patil
Centre for Organized Matter Chemistry, School of Chemistry
University of Bristol, Bristol BS8 1TS (UK)
E-mail: s.mann@bristol.ac.uk
Dr. A. Seddon, Prof. P. Booth
Department of Biochemistry, University of Bristol
Bristol BS8 1TD (UK)

[**] We thank EPSRC for financial support.

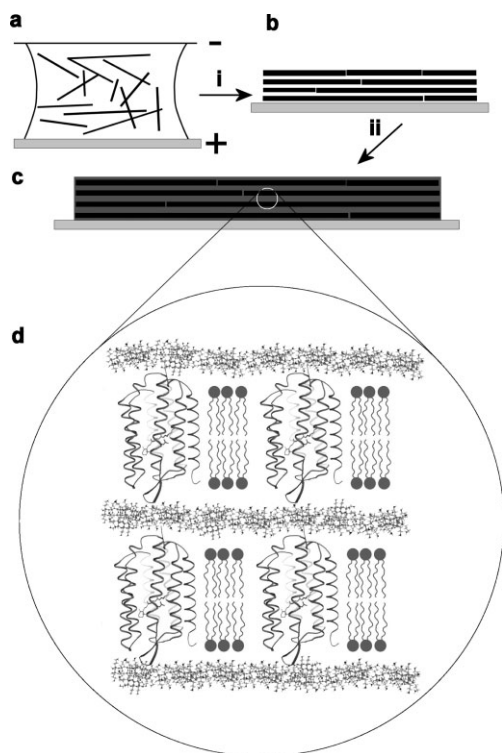


Figure 1. Schematic showing general approach to the fabrication of BR-containing mesolamellar nanocomposites. a) Aqueous dispersion of PM fragments in applied electric field (25 V cm^{-1}); electrophoretic deposition results in oriented stacking of PM fragments on the tin oxide-coated glass slide (anode) (step i). b) Air-dried PM film with lamellar structure (interlayer spacing, 5 nm); swelling of the film with an aqueous solution of prehydrolysed aminopropyltriethoxysilane followed by slow evaporation at controlled relative humidity gives rise to silica intercalation within the interlayer spaces (step ii). c) Mesolamellar organosilica/PM nanocomposite with expanded interlayer spacing (7.6 nm); the self-supporting film exhibits photoelectric and photochromic properties due to entrapment of functionally intact BR molecules. d) Structural model (side view) of mesolamellar hybrid nanocomposite showing interlayer intercalation of silica nanosheets between two adjacent PM bilayer lipid membranes containing oriented BR molecules. Analogous mesolamellar structures containing intercalated organoclay or polymer components were prepared by employing appropriate reaction solutions in step ii.

the presence of various aqueous solutions (see experimental methods). For example, organosilica/PM lamellar nanocomposites were readily prepared by swelling an electrophoretically deposited film of oriented PM fragments with a droplet of prehydrolysed aminopropyltriethoxysilane (APTES), followed by slow drying in air at constant relative humidity. Similar procedures were employed to produce BR-containing mesolamellar composites containing nanometre-thick layers of intercalated aminopropyl-functionalized magnesium phyllosilicate by using an aqueous solution of the organoclay oligomers. Likewise, polymer/BR mesolamellar films were prepared by swelling PM films in the presence of aqueous solutions of PVA, poly-L-lysine or the cationic polysaccharide, chitosan. In each case, the bioinorganic or polymer-containing composite materials were produced as intact, self-supporting structures (Fig. 2a), which were stable when immersed in dis-

tilled water for several months. In contrast, non-intercalated PM films were extremely brittle when dried, and readily solubilized in water.

SEM images of the nanocomposites (Fig. 2b–f) showed continuous and smooth films that were between 5 and 15 μm in thickness depending on the conditions of deposition. Compared with PM films, which were extensively fragmented when imaged by SEM, the composite films were significantly more flexible. In each case, energy dispersive x-ray (EDX) analyses confirmed the presence of phosphorus and sulphur associated with the lipids and proteins of the stacked PM fragments. In addition, strong peaks for Si, or Si and Mg, were detected for the organosilica and organoclay-containing composites, respectively, and elemental mapping of these films viewed in cross-section showed a homogeneous distribution of the intercalated inorganic phases (data not shown).

Powder X-ray diffraction (XRD) studies on electrophoretically deposited PM films showed a characteristic sharp peak at low angle ($2\theta = 1.77^\circ$) (Fig. 3a(i)), which corresponded to a lamellar structure with an interlayer reflection (d_{001}) of 5 nm, and was commensurate with the known PM bilayer thickness.^[13] A second order reflection at d_{002} was observed at 2.5 nm (data not shown), and indicated that well-ordered PM films could be routinely generated by electrophoretic deposition. In contrast, the d_{001} reflection at 5 nm was completely eliminated in XRD profiles recorded for PM films intercalated with solutions of prehydrolysed APTES prepared at an organosilica:PM mass ratio of ~ 0.75 ; instead, a broad reflection was observed at $2\theta = 1.51^\circ$, corresponding to an expanded d_{001} value of 7.6 nm (Fig. 3a(ii)). The associated expansion of 2.6 nm in the interlayer spacing was attributed to the formation of a bioinorganic lamellar mesostructure, and indicated that evaporation-induced condensation of organosilica occurred specifically within the inter-membrane hydration layers of the swollen PM film. No second-order lamellar reflection was observed indicating that the stacking order was disrupted to some extent during silica intercalation.

Similar XRD results were obtained for PM-based composites prepared in the presence of organoclay oligomers (Fig. 3a(iii)), or various organic macromolecules such as chitosan (Fig. 3a(iv)), polyvinyl alcohol (Fig. 3a(v)) or poly-L-lysine (Fig. 3a(vi)). In each case, the XRD profiles were consistent with the formation of a partially disordered hybrid mesolamellar film with expanded interlayer spacings of 5.9, 5.9, 6.0, and 6.9 nm, respectively. Although the thickness of the intercalated polymer layers was generally less than 2 nm, the mean width of the intercalated sheets of organosilica could be increased from 1 to 4 nm by increasing the organosilica:PM mass ratio from 0.5 to 2.5 (Fig. 3b). Organosilica/PM films fabricated at higher mass ratios up to a value of 2.5 had constant interlayer spacings of 8 nm. Samples prepared above this value did not show any evidence in the XRD patterns for the formation of a mesolamellar structure. Instead, under these conditions the relatively high concentrations of hydrolysed organosilica precursors resulted in bulk precipitation of bio-inorganic components.

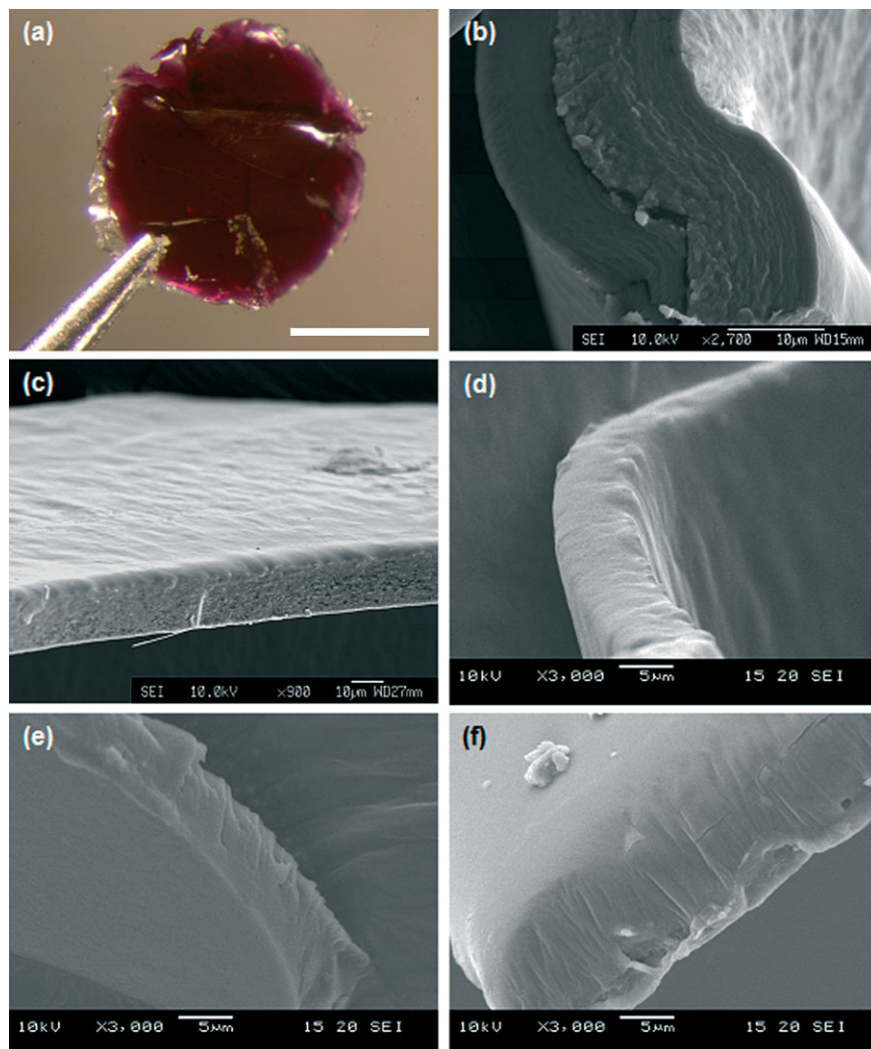


Figure 2. Hybrid mesolamellar nanocomposites prepared by intercalation of guest materials into PM films. a) Optical micrograph showing intact film of an organosilica/PM nanocomposite held between tweezers after removal from an electrode substrate (scale bar = 1 mm). b)–f) SEM images of b) organosilica/PM, c) organoclay/PM, d) polyvinyl alcohol/PM, e) polylysine/PM, and f) chitosan/PM mesolamellar films.

Formation of the organosilica/PM lamellar mesostructure was confirmed by TEM investigations using samples prepared by focused ion beam milling. High magnification images of materials prepared at an organosilica:PM mass ratio of 0.75 showed well-defined lattice fringes with a periodicity of (7.4 ± 0.5) nm (Fig. 3c), in good agreement with the XRD data. The silica layers were imaged as 2.5 nm-thick electron dense stripes, and were separated by 5 nm-wide bands of low contrast, each of which corresponded to a lipid bilayer sheet and associated BR molecules.

The structural integrity of the BR molecules entrapped within the various types of fabricated mesolamellar PM-containing nanocomposites was assessed by FTIR and UV/Vis spectroscopies. In all cases, characteristic amide I ($C=O$ str, 1659 cm^{-1}) and amide II ($N-H$ def; $C-N$ str, 1545 cm^{-1}) absorption bands were observed, indicating that the helical

secondary structure of BR was preserved in the hybrid films. Vibration modes corresponding to the formation of condensed frameworks of organosilica ($Si-C$ (1122 cm^{-1}), $Si-O-Si$ (1035 cm^{-1}), terminal $-NH_3^+$ (3039 cm^{-1})), or organoclay ($Mg-O$ and $Mg-O-Si$ (580 cm^{-1}), $Si-O-Si$ (990 cm^{-1}), and $Si-C$ (1066 cm^{-1})) were also observed in the respective composites, confirming that condensation of the inorganic frameworks within the interlayer spaces of the PM film occurred during evaporation-induced drying of the intercalated samples. UV/Vis spectra of the bioinorganic or polymer-containing nanocomposites showed no significant shift in the characteristic 567 nm absorption band of the retinal chromophore of BR, indicating that the structural and dynamical properties of the membrane-bound protein were retained within the mesolamellar films.

Retention of biofunctionality was also consistent with preliminary studies of the photochromic properties of the hybrid films. Typically, PM films, as well as each of the different types of nanocomposite, showed no visible long-lasting chromatic change on irradiation by white light or using a 632.8 nm HeNe when prepared at pH 7. In contrast, reversible bleaching of the purple ground state to produce a yellow coloration was observed for all samples prepared or post-treated at pH 9, indicating that stabilization of the unprotonated M state at high pH could be readily achieved in the hybrid mesolamellar films. Interestingly, the aminopropyl-functionalized clay and organosilica-containing nanocomposites showed pro-

longed stabilization of the M state when compared qualitatively with native PM or polymer-intercalated films, suggesting that the high pK_a of the covalently linked amino moiety facilitated buffering of the local pH at the surface of the intercalated PM lipid bilayers.

The photovoltaic properties of the organosilica/PM films were investigated by irradiation of the samples at a wavelength of 633 nm under different conditions (experimental methods). The nanocomposites showed typical light-on and light-off photoelectric signals analogous to those observed for PM films (Fig. 4a), indicating that the BR molecules remained functionally active within the mesolamellar structure. Significantly, under optimum conditions (pH 7, 25% relative humidity), the light-on response signal for native and organosilica/PM films were approximately +30 and +60 mV respectively (Fig. 4b). Similarly, the magnitude of the light-off signal

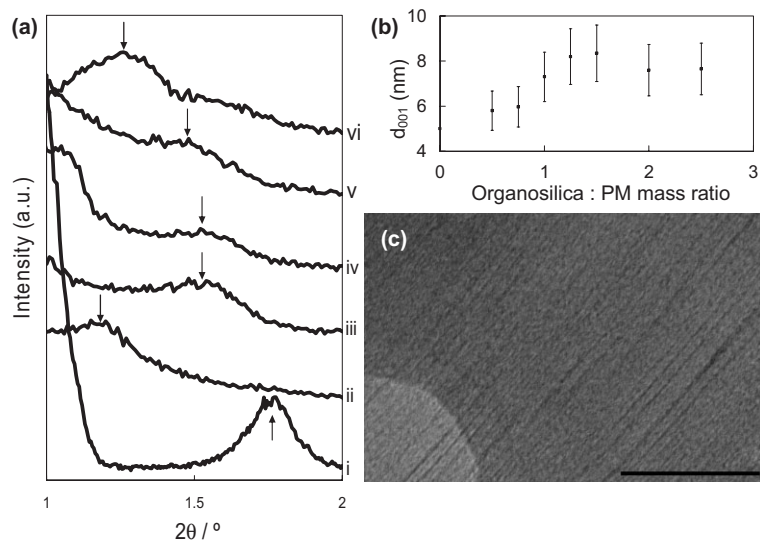


Figure 3. Structural studies on hybrid PM-based nanocomposite films. a) XRD profiles showing low angle peaks (arrows) corresponding to ordered mesolamellar phases for (i) native PM, (ii) organosilica/PM, (iii) organoclay/PM, (iv) chitosan/PM, (v) polyvinylalcohol/PM and (vi) poly-L-lysine/PM films. b) Plot of d_{001} spacing against organosilica:PM mass ratio, and c) TEM image of showing mesolamellar structure for an organosilica/PM film viewed in cross-section (scale bar = 100 nm). Corresponding EDX analyses (not shown) revealed the presence of Si, as well as P and S, associated with inorganic and lipid components, respectively.

and corresponding time constant (~ 10 seconds) were significantly larger for the mesolamellar composite films compared with unmodified PM films. Moreover, increasing the relative humidity to 50% had negligible effect on the light-on response of the bioinorganic composite, whereas the unmodified PM films displayed a marked reduction in the photovoltaic signal to a value of +10 mV (Fig. 4c).

The enhanced photovoltaic response of the mesolamellar hybrid structure at 25% relative humidity suggests an increased proton conductance possibly via hydrogen bonded water molecules associated with $-\text{SiOH}$ groups of the intercalated silica nanosheets. Sol-gel derived porous glasses are known to conduct H^+ ions at high water content in humid atmospheres by proton hopping between SiOH groups and trapped molecular water.^[25,26] In addition, or alternatively, intercalation of the nanometre-thick layers of silica between the oriented PM fragments could reduce the ionic back-current that is known to occur via water molecules located at defects in the PM stack or at the edges of the film.^[27] Increasing the relative humidity to 50% virtually eliminated the photoelectric response of PM films, presumably because of the increased passive backward flow of protons^[27] but had minimal effect on the value of the photovoltage maintained across the organosilica/PM mesolamellar film. These observations support the notion that increased structural integrity in the laminated hybrid materials via the interleaving of nanosheets of silica and lipid bilayers is responsible for the retention in bio-functionality at 50% relative humidity by reducing the proton counter-flow. However, we cannot rule out the possibility that the extent of hydration at the

surface of the lipid membranes remains effectively unchanged on increasing the relative humidity due to high localised hygroscopy associated with the layers of intercalated silica.

In summary, we have demonstrated a simple procedure based on the swelling/drying of electrophoretically deposited PM films for the fabrication of BR-containing hybrid lamellar mesostructures. The bio-nanocomposites consist of periodic sheets of uniformly oriented PM lipid bilayers sandwiched by nanometre-thick layers of amorphous silica, and show an increased and sustained photoelectric response under conditions of high relative humidity when compared with unmodified PM films. Such observations offer significant promise for the development of robust functional BR-based lamellar nanocomposites for integration into a wide range of novel electronic devices and optical storage systems. Furthermore, we have also shown that the fabrication method can be readily extended to produce a range of novel BR-containing hybrid mesolamellar films with intercalated inorganic (organoclay) or organic (polyvinyl alcohol, poly-L-lysine, chitosan) layers, suggesting significant scope for these nanocomposites in numerous biotechnological and biomimetic applications.

Experimental

Purple membrane fragments containing native or mutant BR-D96N bacteriorhodopsin were obtained from MIB (Marburg, Germany) and used without purification. Samples were dispersed in Milli-Q water at a concentration 5.5 mg mL^{-1} ($\text{OD}_{568} = 10$). Electrophoretic deposition of the PM fragments was typically undertaken by placing 20 μL of the PM suspension between a tungsten cathode and a tin oxide-coated glass slide anode separated at a distance of 2 mm [20]. (The electrodes were cleaned by sonication in 50:50 water/acetone mixture and distilled water alone for 15 minutes prior to electrophoretic deposition). A 25 V cm^{-1} electric field was then applied through the droplet until a purple film appeared on the surface of the anode. Excess solution was carefully removed and the film left to dry in air.

Preparation of Organosilica/PM Nanocomposites: Aminopropyl-functionalized (AMP) silica/PM lamellar nanocomposite films were obtained by placing a 20 μL droplet of a prehydrolysed silica precursor solution prepared at pH 7 on top of a freshly prepared electrophoretically deposited PM film and allowing the droplet to slowly evaporate in a chamber above 70% relative humidity (RH) at room temperature. The droplet was typically left overnight to completely evaporate. The prehydrolysed AMP-silica solution was prepared by mixing 5 mL of 3-aminopropyltriethoxysilane (3-APTES) (Sigma) with 20 mL of 0.5 M hydrochloric acid followed by addition of appropriate amounts of distilled water, removal of ethanol by vacuum distillation in a rotary evaporator at 45°C , and adjustment of the pH to 7 with 0.5 M hydrochloric acid. Films were prepared using a range of AMP-silica precursor concentrations (0.01 M to 0.1 M), corresponding to organosilica: PM mass ratios from 0.25 to 2.5.

Preparation of Polymer/PM Nanocomposites: Polymer/PM nanocomposite films were prepared by a similar procedure as above. Dried PM films were produced by passive deposition and swollen using various aqueous polymer solutions, and then air-dried. Solutions of chitosan (Aldrich, low molecular weight, in 1% acetic acid), poly-L-lysine

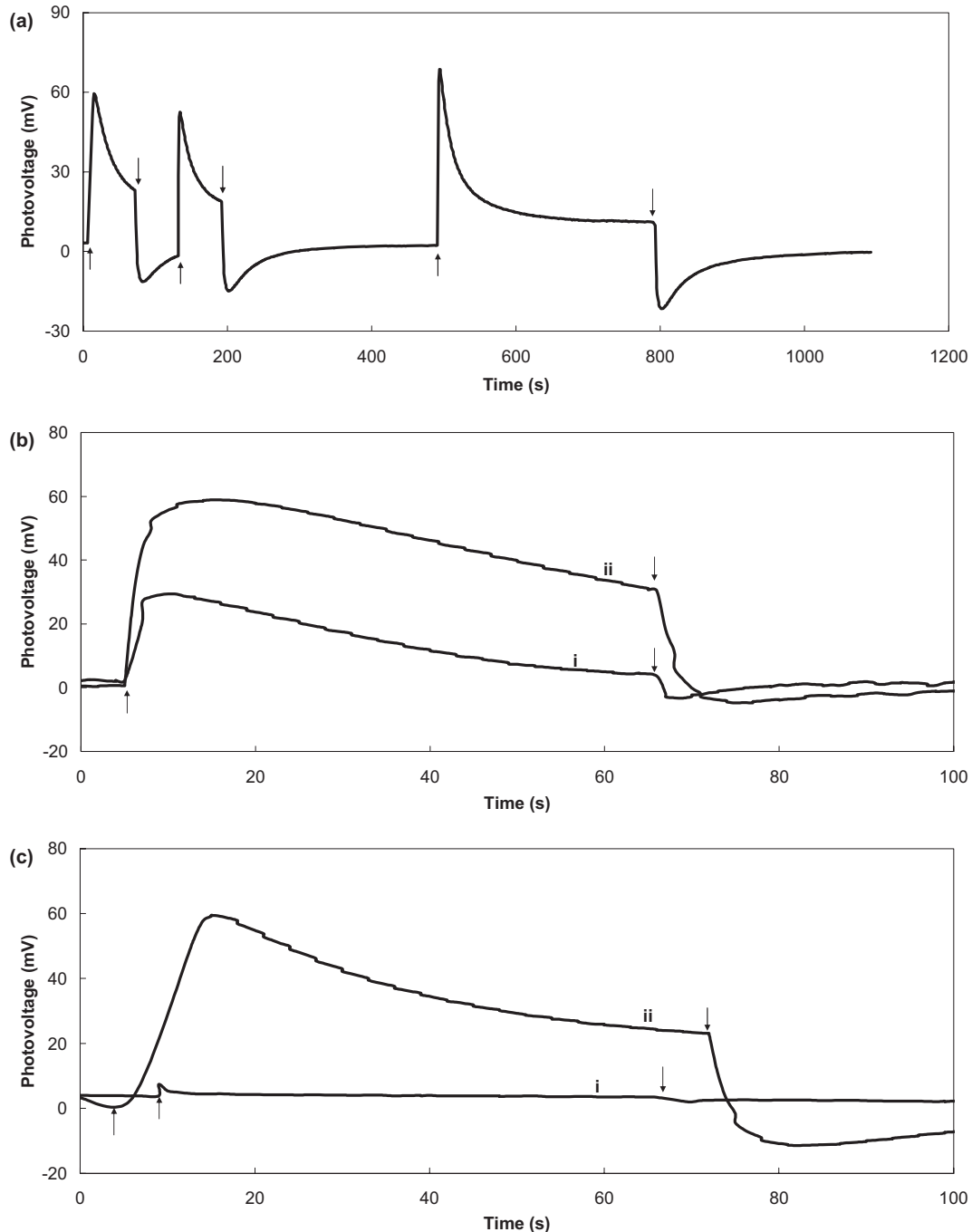


Figure 4. Photovoltaic response studies for organosilica/PM mesolamellar nanocomposites. Upwards arrow indicates “light on” and downwards arrow indicates “light off” in all graphs. a) Plot of voltage against time showing three photoresponse cycles from an organosilica/PM nanocomposite recorded at 50% relative humidity. b) and c) Comparison of photovoltaic responses for (i) PM film (control) and (ii) organosilica/PM mesolamellar nanocomposite at (b) 25% relative humidity, and (c) 50% relative humidity.

(Sigma, molar mass = 500–2000 g mol⁻¹) and polyvinyl alcohol (Sigma, molar mass = 85 000–146 000 g mol⁻¹) were used at polymer:PM mass ratios from 0.05 to 1. An optimum mass ratio of 0.2 (corresponding to polymer concentrations of ca. 1 mg mL⁻¹) was used predominantly for successful intercalation of each of the polymers.

Preparation of Organoclay/PM Nanocomposites: AMP-functionalized magnesium phyllosilicate/PM lamellar films were fabricated

using a similar protocol as described above but using an aqueous solution of organoclay cationic oligomers to swell the deposited PM films. Hybrid films were prepared using a range of organoclay oligomers:PM mass ratios from 0.25 to 1. A mass molar ratio of 0.75 was typically used to prepare highly-ordered organoclay-PM hybrid films. The oligomeric organoclay solution was prepared as described previously by exfoliation of a colloidal dispersion of AMP-functionalized

magnesium phyllosilicate clay [28]. In brief, 100 mg of a dried AMP-clay was dispersed in distilled water (10 mL), ultrasonicated for 5 min, and the resulting cloudy dispersion passed through a sephadex G-25/75 column (Aldrich) to produce a clear eluate of soluble organo-clay oligomers at a concentration of 5 mg mL⁻¹. The AMP-clay was synthesized at room temperature as described previously [28] by dropwise addition of 3-APTES (1.3 mL, 5.85 mmol) to an ethanolic solution of magnesium chloride (0.84 g, 3.62 mmol) in ethanol (20 g), to give a white slurry that was stirred overnight, and then isolated by centrifugation, washed with ethanol (50 mL) and dried at 40 °C.

Photoelectric Studies: For photoelectric measurements, square patches of gold were deposited onto PM control films and AMP-silica-PM films. The patches of gold were each connected to a 0.1 mm platinum wire using colloidal silver conductive paint. The connection was further strengthened with a small amount of Araldite epoxy resin superglue. The platinum wire and TO electrode were connected via an earthed, screened cable to a voltmeter (UNI-T UT70B), which was in turn connected to a computer to record the potential difference across the film. The film was placed in an earthed aluminium foil coated chamber, in which the humidity could be controlled. The film was then irradiated with a 632.8 nm He-Ne laser (Melles Griot) with a 5 mW mm⁻² output and the photovoltage recorded. The photovoltaic signals were recorded at optimized pH~7 and by varying RH. The RH (25 and 50 %) was regulated by placing humidity sensor (Honeywell—IH-3602C) in the chamber at the same level as the film. RH was raised by bubbling argon gas through H₂O at varying rates or lowered by passing argon gas directly through the chamber.

Characterization: Samples were characterized by XRD (Bruker-Nonius D8 diffractometer, Cu K α radiation, $\lambda=0.15404$ nm). FTIR spectroscopy (Perkin Elmer Spectrum 1) was carried out by using KBr discs. Absorption spectra were recorded by using Lambda-25, Perkin-Elmer UV/Vis spectrophotometer. Structural and morphological characterization of native PM and organosilica-, organo-clay-, and polymer-PM composite films were performed by using SEM (JEOL, JSM 6330 FEG-SEM) and TEM (JEOL 1200EX) and EDXA facility (Oxford instruments, ISIS 300). Cross-sections of a silica-PM film were obtained by an FIB milling and imaging tool (FEI Strata FIB201) using a micromanipulator to move the cross-section from the sample stage onto a holey carbon coated copper grid for TEM analysis.

Received: October 2, 2006

Revised: March 15, 2007

Published online: August 8, 2007

- [1] E. Katz, I. Willner, *Angew. Chem. Int. Ed.* **2004**, *43*, 6042.
- [2] C. M. Niemeyer, *Angew. Chem. Int. Ed.* **2001**, *40*, 4128.
- [3] N. Hampp, D. Oesterhelt, in *Nanobiotechnology: Concepts, Applications and Perspectives* (Eds: C. M. Niemeyer, C. Mirkin), Wiley-VCH, Weinheim, **2004**.
- [4] a) U. Haupts, J. Tittor, D. Oesterhelt, *Annu. Rev. Biophys. Biomol. Struct.* **1999**, *28*, 367. b) N. Hampp, *Chem. Rev.* **2000**, *100*, 1755. c) N. Hampp, *Appl. Microbiol. Biotechnol.* **2000**, *53*, 633.
- [5] C. Bräuchle, N. Hampp, D. Oesterhelt, *Adv. Mater.* **1991**, *3*, 420.
- [6] Z. P. Chen, A. Lewis, H. Takei, I. Nebenzahl, *Appl. Opt.* **1991**, *30*, 5188.
- [7] J. Y. Huang, Z. P. Chen, J. Lewis, *J. Phys. Chem.* **1989**, *93*, 3314.
- [8] H. H. Weetall, B. Robertson, D. Cullin, J. Brown, M. Walch, *Biochim. Biophys. Acta* **1993**, *1142*, 211.
- [9] S. G. Wu, L. M. Ellerby, J. S. Cohan, B. Dunn, M. A. El-Sayed, J. S. Valentine, J. I. Zink, *Chem. Mater.* **1993**, *5*, 115.
- [10] H. H. Weetall, *Appl. Biochem. Biotechnol.* **1994**, *49*, 241.
- [11] H. H. Weetall, *Biosens. Bioelectron.* **1996**, *11*, 327.
- [12] T. J. M. Luo, R. Soong, E. Lane, B. Dunn, C. Montemagno, *Nat. Mater.* **2005**, *4*, 220.
- [13] J. A. He, L. Samuelson, L. Li, J. Kumar, S. K. J. Tripathy, *Langmuir* **1998**, *14*, 1674.
- [14] J. A. He, L. Samuelson, L. Li, J. Kumar, S. K. J. Tripathy, *J. Phys. Chem. B* **1998**, *102*, 7067.
- [15] J. A. He, L. Samuelson, L. Li, J. Kumar, S. K. J. Tripathy, *Adv. Mater.* **1999**, *11*, 435.
- [16] S. B. Hwang, J. I. Korenbrot, W. Stoeckenius, *J. Membr. Biol.* **1977**, *36*, 115.
- [17] T. Furuno, K. Takimoto, T. Kouyama, A. Ikegami, H. Sasabe, *Thin Solid Films* **1988**, *160*, 145.
- [18] H. H. Weetall, L. A. Samuelson, *Thin Solid Films* **1998**, *312*, 306
- [19] M. Ikonen, J. Peltonen, E. Vuorimaa, H. Lemmetyinen, *Thin Solid Films* **1992**, *213*, 277.
- [20] G. Váró, *Acta Biol. Acad. Sci. Hung.* **1981**, *32*, 301.
- [21] S. Crittenden, S. Howell, R. Reifengerger, J. Hillebrecht, R. R. Birge, *Nanotechnology* **2003**, *14*, 562.
- [22] K. Koyama, N. Yamaguchi, T. Miyasaka, *Science* **1994**, *265*, 762.
- [23] R. A. Brizzolara, *Biosystems* **1995**, *35*, 137.
- [24] A. M. Seddon, H. M. Patel, S. L. Burkett, S. Mann, *Angew. Chem. Int. Ed.* **2002**, *41*, 2988.
- [25] M. Nogami, R. Nagao, C. J. Wong, *J. Phys. Chem. B* **1998**, *102*, 5772.
- [26] M. Nogami, *J. Phys. Chem. B* **2001**, *105*, 4653.
- [27] K. Uehara, K. Kawai, T. P. Kouyama, *Thin Solid Films* **1993**, *232*, 271.
- [28] A. J. Patil, E. Muthusamy, S. Mann, *Angew. Chem. Int. Ed.* **2004**, *43*, 4928.